

# Augmented Environment Representations with Complete Object Models

Krishnananda Prabhu Sivananda, Francesco Verdoja, Ville Kyrki

**Abstract**—While 2D occupancy maps commonly used in mobile robotics enable safe navigation in indoor environments, in order for robots to understand and interact with their environment and its inhabitants representing 3D geometry and semantic environment information is required. Semantic information is crucial in effective interpretation of the meanings humans attribute to different parts of a space, while 3D geometry is important for safety and high-level understanding. We propose a pipeline that can generate a multi-layer representation of indoor environments for robotic applications. The proposed representation includes 3D metric-semantic layers, a 2D occupancy layer, and an object instance layer where known objects are replaced with an approximate model obtained through a novel model-matching approach. The metric-semantic layer and the object instance layer are combined to form an augmented representation of the environment. Experiments show that the proposed shape matching method outperforms a state-of-the-art deep learning method when tasked to complete unseen parts of objects in the scene. The pipeline performance translates well from simulation to real world as shown by  $F_1$ -score analysis, with semantic segmentation accuracy using Mask R-CNN acting as the major bottleneck. Finally, we also demonstrate on a real robotic platform how the multi-layer map can be used to improve navigation safety.

## I. INTRODUCTION

In recent years, we have witnessed great advances in computer vision which have given robots the ability to understand the world around them like never before [1], [2]. At the same time, advances in control of mobile platforms have enabled robots from quadrupedal robot dogs to drones to move in different environments and react to unpredicted circumstances with high reliability.

However, when considering a mobile robot’s ability to perform advanced high-level tasks in unstructured human-inhabited environments, there is a crucial bottleneck stifling the ability of these sensing and acting breakthroughs to lead to the desired level of autonomy, performance, and interaction: the way robots reason on this rich perceptual knowledge is still very limited. When considering navigation for example, ground robots still rely on 2D occupancy maps built using Simultaneous Localization and Mapping (SLAM) algorithms for path planning and obstacle avoidance. These maps are built using only laser scanners and the rich information coming from the variety of visual sensors available to modern robots is mostly ignored. The combination of these sensors would allow the robot to formulate a better

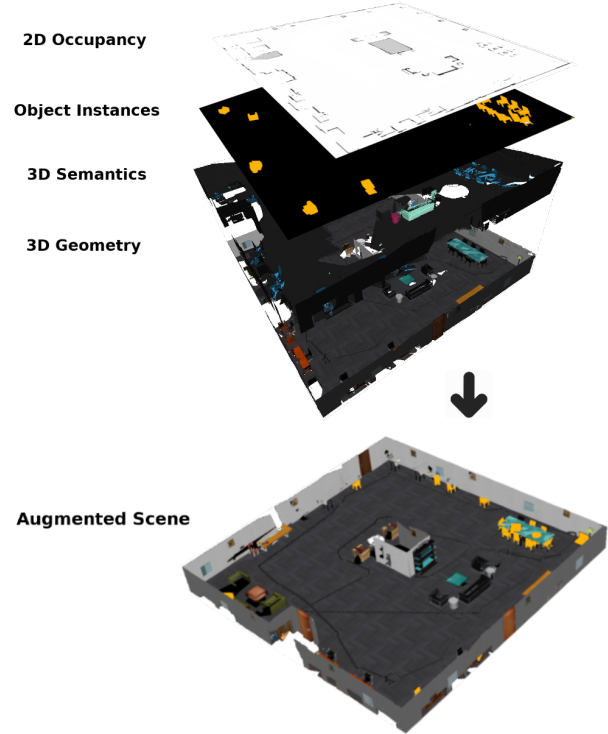


Fig. 1: An environment representation built using the proposed framework.

understanding of its surroundings and, in the case of navigation, to take more intelligent choices to plan its route, *e.g.*, by avoiding obstacles invisible to the laser scanner. Similarly, while interacting with humans, understanding object semantics is crucial for understanding commands in everyday language [3]; having a richer understanding of the environment opens the door for complex capabilities such as mobile manipulation and natural user interaction.

Though methods exist in literature to construct a meaningful 3D representation of the environment [4]–[6], the acquisition of a full 3D map of an environment is a time-consuming process. In most realistic scenarios, the underlying geometry reconstructed by these methods is often incomplete, due to time concerns, occlusions, or environmental traversability limitations affecting the perception of the scene during the mapping process. However, partial geometry is a considerable drawback in some applications; for example, when a robot has to interact with an object, the lack of knowledge of complete geometry can pose safety risks either to the object, the surroundings, or the robot itself. Moreover, complete objects model are also essential for user immersion and safe

K. P. Sivananda is with Cargotec Oy, F. Verdoja and V. Kyrki are with the School of Electrical Engineering, Aalto University, Finland.

The work was conducted while K. P. Sivananda was a student at the School of Electrical Engineering, Aalto University, Finland.

For contacts: francesco.verdoja@aalto.fi

navigation in telepresence applications [7].

In this paper, we propose a mapping pipeline to construct 3D metric-semantic environment representations which include estimates of the full extent of objects in the environment through object shape completion. An example of this representation is shown in Fig. 1. We also propose a novel deterministic approach based on matching (and potential replacement) of a partial object with a similar synthetic model from a known database, which avoids the unpredictability of recent deep-learning-based shape completion approaches. In the experiments, we validate our approach by comparing it to a state-of-the-art deep-learning-based approach for shape completion of chairs.

To summarize, the contributions of this paper are:

- A pipeline to generate a 3D metric-semantic mesh representation of an environment that completes partial objects with similar complete synthetic models.
- Design and evaluation of a novel method to compare and match partial observations of 3D object instances against a database of synthetic models and to replace the partial 3D mesh with the matched model in the reconstructed 3D mesh of the environment.
- Evaluation and comparison of a learning-based approach to complete partial observations of 3D object instances against our proposed method.
- A demonstration of benefits of the proposed environment representation in a 2D navigation case on a real TurtleBot 3 Waffle.

## II. RELATED WORK

Building environment representations where complete models of objects are estimated requires first reconstructing the 3D geometry of the environment, understanding its semantics, and then shape-completing each object instance. In this section, we will review state-of-the-art relevant to these fields, together with relevant works in multi-layer mapping for robots.

*Reconstruction of 3D geometry:* The availability of inexpensive RGB-D cameras such as Kinect has resulted in profound advances in developing 3D reconstruction methods. KinectFusion [4] popularised Truncated Signed Distance Function (TSDF)-based reconstructions as capable of real-time reconstruction of small environments. The main drawback of KinectFusion is the use of a fixed-size voxel grid which requires the map size to be known and a large amount of memory. Multiple extensions have been proposed to address these shortcomings [8], [9]. Among these, Nießner *et al.* [10] propose a spatial hashing scheme to compress space while allowing real-time access and updates of underlying surface data. This spatial hashing was faster than the hierarchical grid data structure used in other methods, however, it relies heavily on GPUs for real-time performance. By exploiting the spatial hashing technique employed in [10], Voxblox [5] focused on improving memory efficiency and real-time performance on the CPU by building incremental Euclidean Signed Distance Fields (ESDFs) from TSDFs. This makes Voxblox able to reconstruct large scale scenes

with reasonable computational costs. In this work, since we are interested in building 3D model of complete environments, we employ Voxblox in the geometric reconstruction module.

*Semantic reconstruction:* The recent innovations in image segmentation methods enabled semantic knowledge to be incorporated into 3D reconstructions into so called semantic-metric representations. Among the methods to perform 3D semantic mapping, SemanticFusion [6] combines the real-time SLAM system ElasticFusion [11] and a CNN for object detection with a Bayesian update scheme for semantic label integration, Voxblox++ [12], an extension of Voxblox, combines geometric segmentation of depth data with instance segmentation by Mask R-CNN [1]. A data association strategy keeps track of labels to ensure global consistency. On the same line, Kimera-Semantics [13] uses Voxblox allowing however flexibility for choice for the 2D instance segmentation algorithm. It runs faster than [12] and shows accurate reconstruction when compared against ground-truth. In this work, we employ Kimera-Semantics with Mask R-CNN to build semantic representations.

*Shape completion:* Shape completion is the process for inferring a full 3D model of an object based on a partial measurement. Two main approaches to the problem exist: model-matching and generative. Model-matching methods attempt at matching a partial view to a similar model. The most recent example of this class of methods is Scan2CAD [14] which uses a 3D CNN trained on a custom dataset to learn joint embedding between real and synthetic 3D models to predict accurate correspondence heatmaps between model and scan. It requires entire 3D scan of a scene as input and tries to find the alignment of models of all the objects in the scene. The method, however, does not utilize any semantic information of the scene. Recently, generative deep learning methods for shape completion have attracted increasing interest in the community. Although methods working on voxel data exist [15], point-clouds are better suited to represent objects at different resolution. Among the methods working on point-clouds [16]–[18], one of the best performing ones is Point Completion Network (PCN) [2], a shape completion method based on the PointNet architecture. It is capable of generating high-resolution completions and shows generalization over unseen objects and real-world data. However, most of the results presented in works on deep learning shape completion only pertain synthetic data and their ability to transfer from synthetic-partial data to real data has been questioned [17]. Moreover these methods often do not account for much input noise while training. The problem of scene completion (*i.e.*, shape-completing all objects in a scene) is less explored and in that context, which we target in this work, errors in semantic segmentation or geometric reconstruction of the scene can further increase the transfer gap and lessen the performance of deep learning methods even more. In this work, we explore the ability of PCN to transfer to noisy real data as well as propose a novel model-matching approach for scene completion and augmentation.

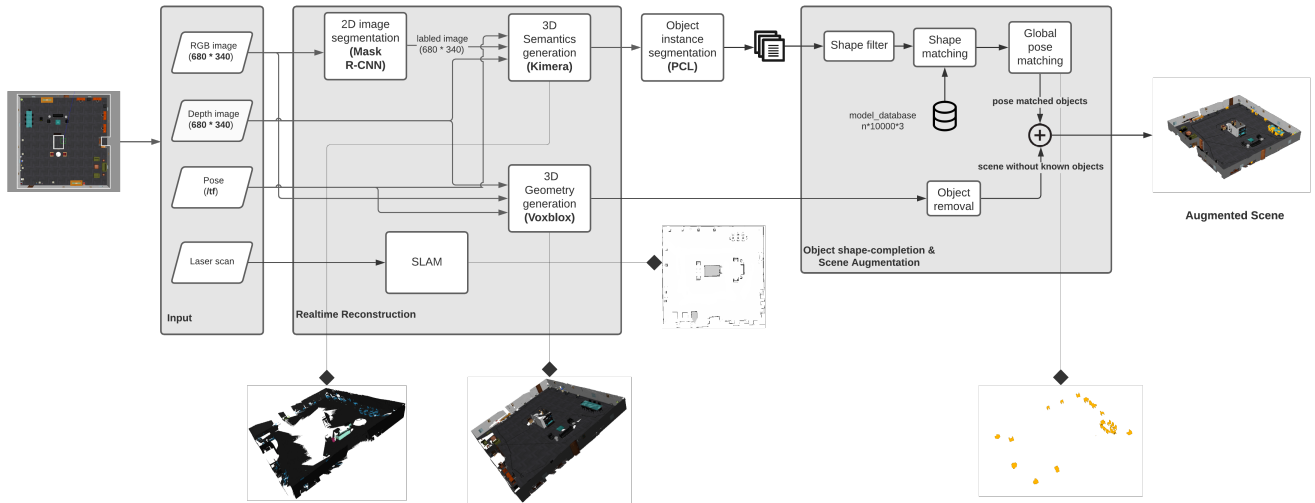


Fig. 2: Detailed overview of the pipeline

*Multi-layer mapping:* Multi-layer maps for robotics are not a new concept. Many works have proposed hierarchical mapping methods where a 2D occupancy map is maintained together with traversability graphs and topology [19], [20]. However, these architectures rarely include multiple maps capturing the environment as seen by different sensor modalities but rather abstract the environment to facilitate reasoning and human-robot interaction.

Recently, motivated by the advancements in computer vision and machine learning, interest has increased toward multi-layer mapping formalisms able to include different sensor information. In [21] a 2D multi-layer mapping framework composed of a metric, semantic, and exploration layers is proposed, and its application in the context of autonomous semantic exploration is presented. In that work, the focus is left on 2D mapping only, and no object shape completion is attempted. Rosinol *et al.* [22] propose a hierarchical graph comprised of multiple layers, including one where object extents are estimated by fitting a CAD model to the partial object. In this work, we propose a more general approach to shape completion, by matching over a database of object models, instead of a single one.

### III. PROBLEM FORMULATION

The aim of this work is to build rich map representations where geometric information of the environment is maintained together with the object semantics. Additionally, we want to maintain an estimate over the full extent of each object.

Formally, we want to build a hierarchical multi-layer map  $\mathcal{M} = \{\mathbf{M}, \mathbf{G}, \mathbf{S}, \mathbf{O}\}$ , composed of the following layers:

- 1) 2D geometry  $\mathbf{M}$ : a representation of traversable area, often used for navigation and obstacle avoidance;
- 2) 3D geometry  $\mathbf{G}$ : a representation of the environment where objects can be recognized by their appearance;
- 3) 3D semantics  $\mathbf{S}$ : a representation where semantic information over objects in the environment is maintained;

- 4) Object instances  $\mathbf{O} = \{o^*\}$ : for each object in the environment, we want to estimate its full extent  $o^*$  from a partial view  $\tilde{o}$ .

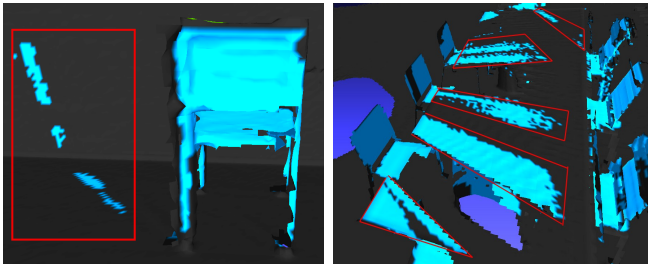
In the next section we will discuss the proposed pipeline, which builds all the aforementioned maps iteratively by means of visual and range information obtained by a robotic platform exploring the environment.

### IV. METHOD

The proposed pipeline, shown in Fig. 2, is split into *Realtime Reconstruction* and *Scene Augmentation*. *Realtime Reconstruction* includes modules to build the geometric and semantic representations. These reconstructions form the input to the second half of the pipeline, that performs *Scene Augmentation* on the input to deliver the final geometric representation of the scene having objects with complete geometry. All representations are kept aligned to a 2D occupancy map  $\mathbf{M}$  built through SLAM. The proposed pipeline consists of the combination of existing software components along with novel components to produce the final representation. While developing the pipeline, the emphasis was kept on the flow of data rather than on the individual component implementations. Hence, each component is independent from the others, thereby easily replaceable with any current or future work that can ensure the same data flow.

#### A. Realtime reconstruction

The purpose of the reconstruction module is to generate the 3D geometric representation  $\mathbf{G}$  and the semantic-geometric representation  $\mathbf{S}$  online. Both layers will be represented as 3D colored meshes; in  $\mathbf{G}$ , each face's color will represent the color information obtained from the camera, while in  $\mathbf{S}$  the color will map to a semantic object class. Semantic information is gathered through a deep learning based pixel-level instance segmentation method, the output of which along with the respective depth image and pose information is used to generate the semantically annotated



(a) Spread onto wall and floor (b) Spread onto a table

Fig. 3: Discrepancies caused by inaccurate object mask. In both pictures the marked regions represent erroneous spread of a label (best viewed in color).

3D mesh. In this work, we use Voxelbox [5] and Kimera-Semantics [13] to construct the geometric and semantic-geometric representation respectively, employing Mask R-CNN [1] as the deep learning algorithm to obtain the object semantic segmentation from images.

This stage outputs  $\mathbf{G}$  and  $\mathbf{S}$ , *i.e.*, a geometric and a semantic-geometric representation of the environment available in a mesh format which are converted to point-clouds due to ease of processing for the latter stage of the pipeline.

### B. Object shape completion and scene augmentation

In order to obtain the object instances to shape-complete, the semantic point cloud is segmented into individual clusters, with each cluster representing a partial view  $\tilde{o}$  of an object  $o$ . Object instances are identified using differences of normals. Then, given a semantic class  $c$ , for each partial view  $\tilde{o}$  for which  $\mathbf{S}(\tilde{o}) = c$ , we propose an object shape-completion method  $f_c$  to estimate its full extent  $o^*$ . Formally,  $f_c : \tilde{o} \rightarrow o^*$ . In this work, we demonstrate the augmentation by replacing chairs, but the proposed methodology can be applied to other classes of objects as well.

1) *Shape Filter*: After clustering, it can happen that some clusters  $\tilde{o}$  may be incorrectly classified to class  $c$ . This can happen *e.g.*, for issues of time synchronization between RGB and depth images, or because the mask obtained from Mask R-CNN may contain parts that do not belong to the object. The marked regions in Fig. 3 are examples of such cases. To avoid completing the shapes of mislabeled objects, we pass each cluster through two filters aiming at recognizing erroneous labeling.

The first filter aims at recognizing label-bleeding along walls and floor by identifying planarity of a cluster point-cloud by its covariance matrix. A cluster is discarded if the covariance matrix shows values close to zeros for at least one of the axes.

The second filter aims at identifying mislabeled objects. Objects of a certain class tend to have similar shape and size, and these can be used to identify objects which do not conform to the class model. In practice, we determined the distance of the farthest point to the object centroid  $\lambda$  and removed objects for which this measure was out of range for any sort of chair commonly found in an office or home

environment. Despite the filtering, some false positives may remain for later stages.

2) *Shape matching*: In order to estimate the full extent of an object, we match its partial shape  $\tilde{o}$  to a similar synthetic model  $o^*$ . Formally, given  $\tilde{o}$ , a partial view of an object of class  $c$ , and  $\mathbf{C} = \{o_i\}_{i=1}^N$ , a database of  $N$  object models  $o_i$  of class  $c$ , we want to find

$$o^* = \arg \min_{o_i \in \mathbf{C}} \delta(o_i, \tilde{o}) \quad (1)$$

for some distance metric  $\delta$ . In this study, a custom point-cloud database of chairs was created from the 6778 3D models available in the ShapeNet dataset [23].

In order to compute the distance  $\delta$ ,  $o_i$  and  $\tilde{o}$  need to first be registered to the same pose.

*Pose matching*: Inferring the pose of an object directly from its raw partial point-cloud representation is quite difficult. Instead, it is easier to find a transformation that can be applied to the model that will align it with the object through point-cloud registration methods through Iterative Closest Point (ICP). However, ICP is a computationally expensive algorithm and is susceptible to getting stuck at local minima, so it is best if any initial estimate of the transformation is available to loosely align the source (database models) with the target (partial point-clouds). ICP can then fine-tune the coarse transformation in very few iterations to tighten the alignment. Given that the natural pose of any grounded objects will always be around the  $z$ -axis, to find a coarse transformation, a random model from the dataset is selected and a set of uniformly sampled rotations are performed around its  $z$ -axis. The transformation matrix for the rotation yielding the minimum average point-to-point distance is used to initialize the ICP algorithm. ICP fine-tunes this rotation over the  $z$ -axis to provide the final transformation matrix. The advantage of this approach is that it is applicable to any grounded object.

*Model matching*: Finding a match involves searching through the database. The final transformation refined after ICP method is applied to each model and the corresponding point-to-point distance with the partial point-cloud is recorded. This is used as a measure of model distance  $\delta$ . The hypothesis is that the model that most closely resembles the actual object should return the smaller distance. The matched model  $o^*$  in the local frame of the partial object is re-scaled and translated back into the world frame and added to the object representation layer  $\mathbf{O}$ .

3) *Scene augmentation*: Finally, after having built  $\mathbf{G}$ ,  $\mathbf{S}$ , and  $\mathbf{O}$ , we build an augmented scene, *i.e.*, a representation where we replace objects in  $\mathbf{G}$  with their complete counterparts in  $\mathbf{O}$ . While not constituting one of the layers of  $\mathcal{M}$ , this additional *virtual* representation can be used for planning and navigation, as we will show in Sec. V-C. To this end, we construct a merged point-cloud  $\mathbf{A} = (\mathbf{G} \setminus \mathbf{S}) \cup \mathbf{O}$ , where  $\mathbf{S} \subset \mathbf{G}$  is the subset of points of  $\mathbf{G}$  that are within a point-to-point distance threshold  $\epsilon$  from any of the object models in  $\mathbf{O}$ .

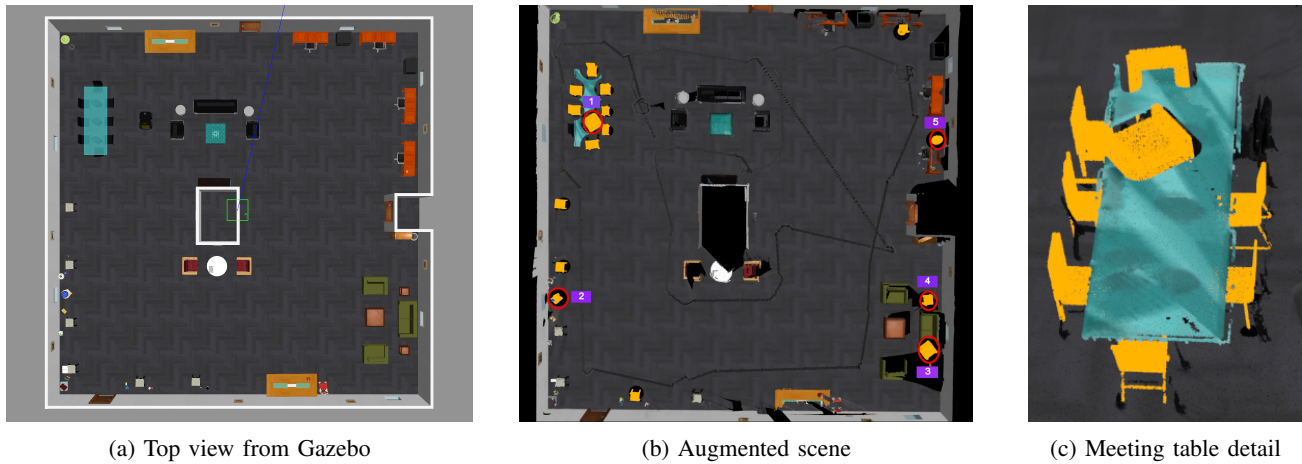


Fig. 4: Simulated office scene (a). In the 3D geometric model (b), chair partial observations have been replaced with the complete models and each area marked in red in (b) denotes a false positive. A detail of the meeting table in the North-West corner of the environment is shown zoomed in (c) (best viewed in color).

## V. EXPERIMENTS

In this section, we present experiments aiming to validate the proposed method by answering the following questions:

- 1) is the pipeline able to reconstruct environments while navigating in them?
- 2) when considering chairs, how reliably can the proposed method locate them and estimate their full extent?
- 3) how does the object extent estimated by the proposed method compare with state-of-the-art shape-completion deep learning methods?

In order to answer these questions we conducted multiple experiments in simulation (Sec. V-A) and on real robotic platforms (Sec. V-B).

As a measure to evaluate the method’s ability to recognize objects, we used the  $F_1$ -score,

$$F_1 = 2 \frac{Precision \cdot Recall}{Precision + Recall}. \quad (2)$$

All experiments have been run on a laptop with Intel Core i7-8750H, 2.20GHz CPU, Nvidia GeForce 1050 Ti GPU, and 16 GB RAM. While they are not presented here due to space limitations, we conducted more experiments that can be found in [24].

Finally, in Sec. V-C, we will demonstrate how the proposed method can improve navigation safety.

### A. Simulation experiment

In order to evaluate the proposed method, we setup a simulated office environment [25] in Gazebo. The environment, shown in Fig. 4a, consists of a few different furnished zones, comprising a meeting table, a couple of lounge areas, and an a few desks. In total, the environment contains 19 chairs distributed among the different zones. 8 chairs around a long meeting table, 6 chairs facing the wall with some objects in between them, 4 office chairs facing one of the desks, and partially slid inside, and one chair near a long table facing the room. We spawn in the environment a simulated model

TABLE I: Experimental results

Experiment	Precision	Recall	$F_1$ -score
Simulated office	0.69	0.59	0.63
Real office	0.71	0.83	0.78
Real corridor	0.80	1.00	0.89

of a Husky robot from Clearpath Robotics, equipped with a Kinect RGBD camera and a SICK laser scanner.

The first aspect we wanted to evaluate in simulation was the ability of the proposed method to correctly identify and then shape-complete the chairs present in the environment. To this end, we manually teleoperated the robot to construct a multi-layer map  $\mathcal{M}$  of the environment using the proposed method. We empirically set the range for  $\lambda$  to  $[0.1, 0.25]$  m, and  $\epsilon = 0.1$  m.

A total of 16 chairs were identified and shape-completed. Out of the 19 chairs in the environment, 11 were correctly identified and the other 5 were false positives. The first row of Tab. I shows the achieved precision, recall, and  $F_1$ -score. The results are quite modest. Misdetections were caused by inaccurate segmentations provided by Mask R-CNN, that were not fully compensated for by the filter described in Sec. IV-B. Fig. 4b provides a top view of the scene after object replacement and the marked objects denote the false positives, and Fig. 4c zooms over the meeting table, where most of the chairs have been completed properly except for one false positive arising from one label spreading on the table top. Mask R-CNN represents current state-of-the-art capabilities in terms of object segmentation, the results presented here are expected to improve with better object segmentation.

Another investigated aspect was the quality of shape-completion produced by the proposed method, in comparison to state-of-the-art deep learning methods. To this end, we compared with PCN [2]. Fig. 5 shows some examples of the output of PCN for chairs mapped at different level of

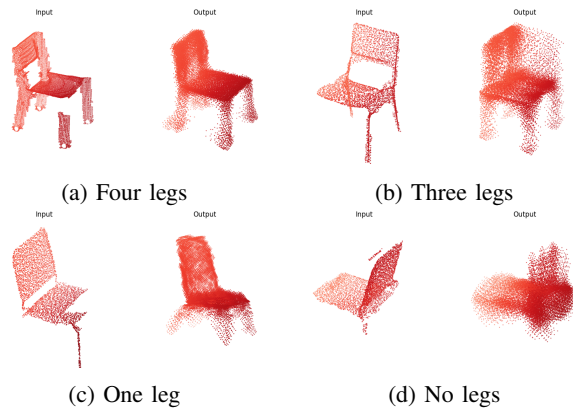


Fig. 5: Performance of PCN on chairs with various degree of completion. Input (left) and output (right) are in the same pose, misalignment is due to a failure of the network.

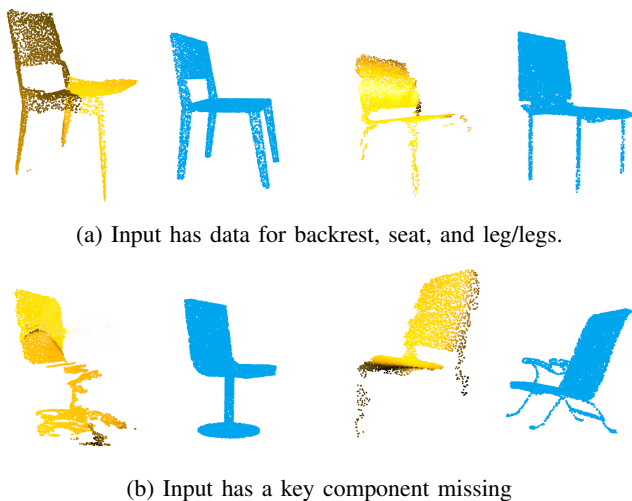


Fig. 6: Matched models using the proposed method. Input point-clouds and model outputs are shown in yellow and blue respectively (best viewed in color).

completion; even when the input is lacking only few regions, the output produced by the network has visible outliers and the internal pose estimation of the network fails. When a similar chair in a different pose as in Fig. 5b is subjected to the network, the confusion of the network is quite evident as it tries to recreate the backrest resulting in a box-like structure above the legs. Fig. 5d and 5c are the same chairs in different orientations. For the former, the network is unable to map it to a chair, whereas for the latter it is not able to infer the extent of legs with one partial leg. All these observations point to the fact that the network performance does not seem to translate to realistic partial views that can be obtained through acquisition “in the wild”.

The errors seen with PCN, *i.e.*, noise and outliers, are not present when using the proposed model matching system. In this case, what influences the output quality is the region of missing information rather than its quantity (Fig. 6). When the input has parts of all the factors that define a chair

which are legs, backrest, seat, and arms a good approximate match is obtained as seen in Fig. 6a. However, when a key component is completely missing from the input, the match may differ significantly from the actual object. In Fig. 6b, we can see that a wheeled office chair lacking arms and the wheeled base in the reconstruction is completed with a circular base instead of a wheeled base (left), while, when only a partial extent of one leg is present (right), the corresponding match found has shorter legs and if this model is placed back in the scene it would hover in the air. The output also has a set of arms that are not present in the actual object. From the observations, it is clear that a complete extent of at least one leg is needed in the input to find a good match that would be properly grounded. However, even when a different chair model is identified as match, the pose and overall shape produced by the proposed method are still consistent with the observed object, which may make these models useful for robotics applications, as demonstrated in Sec. V-C.

### B. Physical experiment

The tests on simulation provided insights into the performance, the factors affecting it, and the bottlenecks in the pipeline. With these limitations in mind, the viability of the pipeline was tested on a Care-O-bot 4 [26] robot produced by Fraunhofer IPA. The robot is equipped with multiple RGBD cameras on the head, neck, and torso to perceive the area in front of it. It is capable of omnidirectional motion with a maximum velocity of 1.1 m/s. Three 2D laser scanners mounted in the base allow the robot to react to static and dynamic obstacles. For the experiments only the RGBD camera mounted in the neck area was used. We mapped two environments using the proposed method: an office where we randomly placed some chairs, and a corridor with chairs along the wall.

1) *Office*: 7 chairs of multiple designs were laid out in a chaotic manner in the room. The robot was teleoperated through the environment for one minute and the environment was mapped with the proposed pipeline using data captured through the RGBD camera mounted in the neck. Fig. 7a shows the environment as reconstructed by the pipeline (layer G), while Fig. 7b shows the augmented scene **A** with the complete object models.

As shown in Tab. I, the setup yielded an  $F_1$ -score of 0.78, significantly better than the simulation. Of the five correctly detected chairs, two (chairs 1 and 4) have good reconstruction quality, and three are reasonable but incomplete: chair 3 because of noise in depth measurements, chair 6 because of inaccurate semantic segmentation, and chair 5 because of heavy occlusion in data. Two false positives were caused by inaccurate semantic segmentation of chair 6. The wheeled base, backrest, and seat were registered whereas the stem connecting the seat with the base was not registered, causing a false positive seen below chair 6. Another false positive was the result of label spreading of Mask R-CNN by which part of the wall behind chair 6 got mislabeled.

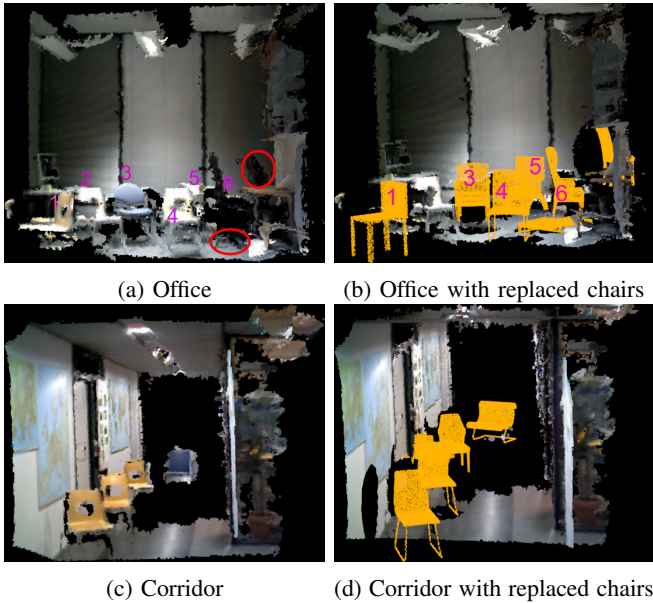


Fig. 7: Pipeline performance

2) *Corridor*: 4 chairs were laid out in a narrow corridor and the robot was immobile in a single observation position. Fig. 7d depicts the result of the pipeline. The  $F_1$ -score of the reconstruction quality was 0.89 (Tab. I), which shows a level of performance above the previous cases. Out of four correct detections, three were accurately reconstructed while one was incomplete due to sensor noise. There was one false positive due to label spreading.

In summary, the inherent shortcomings of Mask R-CNN and label spreading were present also in the real environment. Additionally, it was observed that major occlusions and noise in the depth information influence the quality. However, even if the geometric shape of distant or heavily occluded chairs was inaccurate, their pose was matched quite accurately. Correct pose estimation is a crucial property in robotics, as we will show in the demonstration that follows.

### C. Application: Shape-aware autonomous navigation

As a demonstration of practical usefulness of the multi-layer mapping framework proposed in this work, we explore its use for robotic navigation. Most robots navigate using 2D occupancy maps built using 2D lidar-based SLAM, however those maps only represent occupancy at one specific height and fail to capture the occupancy of complex obstacles. In this demonstration, we custom fitted a Turtlebot3 Waffle Pi robot with a Kinect RGBD camera mounted on a short pole to improve its field-of-view. We setup two environments, shown in Fig. 8a and Fig. 8b, where the robot is on one side of some chairs and has to navigate to the other side. The chair seats provide obstacles for the robot such that if the robot plans a trajectory through the legs of a chair, the pole will collide with a seat.

First, the robot navigated using a 2D lidar-based map and, as can be seen in Fig. 8c and Fig. 8d, the resulting trajectories passed through the chairs and caused a collision.

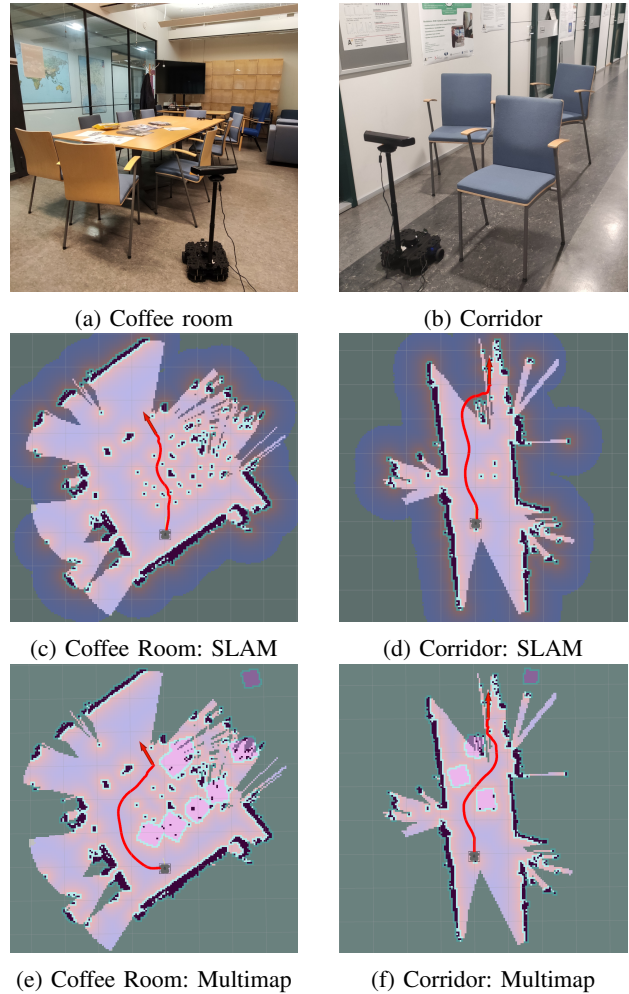


Fig. 8: Navigation experiment results over two scenarios. By navigating using SLAM map only, (c) and (d), the robot collides with chairs, while it avoids all chairs by navigating on the multimap, (e) and (f) (best viewed in color).

Then, estimated object occupancies were projected down to build another 2D costmap, by projecting all points in the object layer having  $z \in [0.1, h]$ , where  $h$  was the height of the robot. Using this map, the robot navigated avoiding all obstacles and reached its destination (Fig. 8e and Fig. 8f).

This demonstration serves first of all to illustrate the usefulness of multi-layer maps that allow integration of information across sensors and map layers. Secondly, it shows how the knowledge maintained by proposed mapping framework can enable reasoning on multiple representations to increase robotic safety, autonomy, and reliability.

## VI. DISCUSSION

Over the past decade, deep learning based image segmentation and shape completion methods have made significant leaps from a computer vision perspective. However, our experiments hint at a problem of applying the current methods in robotics: noisy and incomplete data captured in the wild often deteriorates their performance considerably. This is particularly true for deep learning methods that have usually

hard time to produce reasonable results on out-of-distribution data. In our case, the semantic label from Mask R-CNN was often coarse which led to labels bleeding out of the object boundaries, and required additional post processing steps. As for the methods like PCN, the network training is performed in isolation with existing databases without sufficiently taking the real-world factors into account. Hence, when these models are applied in real world robotic applications, they may fall apart as seen in the experiments. It is important to note that while visual fidelity and quality are important from a computer vision and graphics perspective, when considering robotics, other factors such as precise occupancy and pose may be more crucial.

When considering the proposed method, though it is scalable to account for more object classes, it also adds to the requirement of extensive databases of synthetic models for each object class and the computational overhead to search through those databases to find a match. The process is time consuming for larger environments, but can be performed offline. However, despite all these factors, until deep learning methods improve their ability to transfer, our experiments confirm model matching as the most reasonable choice for object completion for robotics applications.

## VII. CONCLUSIONS

In this paper we presented a multi-layer robotic mapping pipeline able to build in realtime geometric-semantic representation and complete object instances in the environment by model matching. We evaluated the proposed method in both simulation and real environments as well as compared its performance in object shape-completion against a state-of-the-art deep learning method demonstrating how the models produced by our approach are better suited for robotic applications. Finally we demonstrated how the proposed method can be used to increase robustness of navigation. Since the experimental scope was limited to estimating the extent of a single object category, understanding the scalability of the approach requires further studies.

In conclusion, the mapping pipeline presented here represents a step toward mapping methods, where different data sources are combined and artificial intelligence is employed to integrate and complete missing information. More work in this direction is still needed, particularly in regards to bridging the gap between shape completion of synthetic object and scene completion of real environments as well as to explore the inclusion of agent dynamics in the map. However, we believe that such mapping approaches will be pivotal to bring the many recent advances in computer vision to real mobile robot applications.

## REFERENCES

- [1] K. He, G. Gkioxari, P. Dollár, and R. Girshick, "Mask R-CNN," in *IEEE Int. Conf. S on Computer Vision (ICCV)*, 2017, pp. 2980–2988.
- [2] W. Yuan, T. Khot, D. Held, C. Mertz, and M. Hebert, "PCN: Point Completion Network," in *Int. Conf. on 3D Vision*, 2018, pp. 728–737.
- [3] A. K. Pandey and R. Alami, "Towards human-level semantics understanding of human-centered object manipulation tasks for hri: Reasoning about effect, ability, effort and perspective taking," *International Journal of Social Robotics*, vol. 6, no. 4, pp. 593–620, 2014.

- [4] R. A. Newcombe, S. Izadi, O. Hilliges, D. Molyneaux, D. Kim, A. J. Davison, P. Kohi, J. Shotton, S. Hodges, and A. Fitzgibbon, "KinectFusion: Real-time dense surface mapping and tracking," in *IEEE Int. Symp. on Mixed and Augm. Reality*, 2011, pp. 127–136.
- [5] H. Oleynikova, Z. Taylor, M. Fehr, R. Siegwart, and J. Nieto, "Voxblox: Incremental 3D Euclidean Signed Distance Fields for on-board MAV planning," in *2017 IEEE/RSJ International Conference on Intelligent Robots and Systems (IROS)*, 2017, pp. 1366–1373.
- [6] J. McCormac, A. Handa, A. Davison, and S. Leutenegger, "SemanticFusion: Dense 3D semantic mapping with convolutional neural networks," in *2017 IEEE International Conference on Robotics and Automation (ICRA)*, 2017, pp. 4628–4635.
- [7] A. Cesta, G. Cortellessa, A. Orlandini, and L. Tiberio, "Into the wild: Pushing a telepresence robot outside the lab," *Social Robotic Telepresence*, p. 7, 2012.
- [8] T. Whelan, M. Kaess, M. Fallon, H. Johannsson, J. Leonard, and J. McDonald, "Kintinuous: Spatially extended KinectFusion," in *RSS Workshop on RGB-D*, 2012.
- [9] F. Steinbrücker, J. Sturm, and D. Cremers, "Volumetric 3D mapping in real-time on a CPU," *Proceedings - IEEE International Conference on Robotics and Automation*, pp. 2021–2028, 2014.
- [10] M. Nießner, M. Zollhöfer, S. Izadi, and M. Stamminger, "Real-time 3D reconstruction at scale using voxel hashing," *ACM Trans. Graph.*, vol. 32, no. 6, 2013.
- [11] T. Whelan, S. Leutenegger, R. F. Salas-Moreno, B. Glocker, and A. Davison, "ElasticFusion: Dense SLAM without a pose graph," in *Robotics: Science and Systems*, 2015.
- [12] M. Grinvald, F. Furrer, T. Novkovic, J. J. Chung, C. Cadena, R. Siegwart, and J. Nieto, "Volumetric Instance-Aware Semantic Mapping and 3D Object Discovery," *IEEE Robotics and Automation Letters*, vol. 4, no. 3, pp. 3037–3044, 2019.
- [13] A. Rosinol, M. Abate, Y. Chang, and L. Carlone, "Kimera: An open-source library for real-time metric-semantic localization and mapping," in *IEEE Int. Conf. on Robotics and Automation*, 2020, pp. 1689–1696.
- [14] A. Avetisyan, M. Dahnert, A. Dai, M. Savva, A. X. Chang, and M. Niessner, "Scan2CAD: Learning CAD model alignment in RGB-D scans," in *Proceedings of the IEEE/CVF Conference on Computer Vision and Pattern Recognition (CVPR)*, 2019-06.
- [15] A. Dai, C. Ruizhongtai Qi, and M. Nießner, "Shape completion using 3d-encoder-predictor cnns and shape synthesis," in *Proceedings of the IEEE Conference on Computer Vision and Pattern Recognition*, 2017, pp. 5868–5877.
- [16] Z. Huang, Y. Yu, J. Xu, F. Ni, and X. Le, "PF-Net: Point Fractal Network for 3D Point Cloud Completion," in *IEEE/CVF Conf. on Computer Vision and Pattern Recognition*, 2020, pp. 7659–7667.
- [17] X. Chen, B. Chen, and N. J. Mitra, "Unpaired point cloud completion on real scans using adversarial training," in *Int. Conf. on Learning Representations ICLR*, 2020.
- [18] L. P. Tchappmi, V. Kosaraju, H. Rezatofighi, I. Reid, and S. Savarese, "TopNet: Structural point cloud decoder," in *IEEE/CVF Conf. on Computer Vision and Pattern Recognition*, 2019.
- [19] H. Zender, O. M. Mozos, P. Jensfelt, G. J. M. Kruijff, and W. Burgard, "Conceptual spatial representations for indoor mobile robots," *Robotics and Autonomous Systems*, vol. 56, no. 6, pp. 493–502, 2008.
- [20] J. Crespo, R. Barber, and O. M. Mozos, "Relational Model for Robotic Semantic Navigation in Indoor Environments," *Journal of Intelligent & Robotic Systems*, vol. 86, no. 3, pp. 617–639, 2017.
- [21] T. Zaenker, F. Verdoja, and V. Kyrki, "Hypermap mapping framework and its application to autonomous semantic exploration," in *IEEE Int. Conf. on Multisensor Fusion and Integration*, 2020, pp. 133–139.
- [22] A. Rosinol, A. Gupta, M. Abate, J. Shi, and L. Carlone, "3D Dynamic Scene Graphs: Actionable Spatial Perception with Places, Objects, and Humans," *arXiv:2002.06289 [cs]*, 2020.
- [23] A. X. Chang, T. Funkhouser, L. Guibas, P. Hanrahan, Q. Huang, Z. Li, S. Savarese, M. Savva, S. Song, H. Su, J. Xiao, L. Yi, and F. Yu. (2015) ShapeNet: An information-rich 3D model repository.
- [24] K. P. Sivananda, "Semantic mapping for indoor robotics," Master's thesis, Aalto University, Finland, 2020.
- [25] A. Rasouli and J. K. Tsotsos. The Effect of Color Space Selection on Detectability and Discriminability of Colored Objects.
- [26] R. Kittmann, T. Fröhlich, J. Schäfer, U. Reiser, F. Weißhardt, and A. Haug, "Let me introduce myself: I am Care-o-Bot 4, a gentleman robot," in *Mensch Und Computer 2015*, 2015, pp. 223–232.